International Journal of Science and Research Archive
eISSN: 2582-8185
Cross Ref DOI: 10.30574/ijsra
Journal homepage: https://ijsra.net/

(RESEARCH ARTICLE)

Check for updates

Geoelectrical resistivity mapping for sustainable groundwater management in Umuahia South: Insights from vertical electrical sounding

Stephen Obioma Akidi [1], Bridget Odochi Ubechu [2,*], Young Ezenwa Obioha [2], Chigozie Chukwuemeka Ikechukwu [3] and Chinyere Caroline Amadi [2]

[1] *Department of Geology, College of Physical and Applied Sciences, Michael Okpara University of Agriculture, Umudike, Abia state, Nigeria.*
[2] *Department of Geology, School of Physical Sciences, Federal University of Technology, Owerri, Nigeria.*
[3] *GIS Grandmaster Co. Limited Lagos, Nigeria.*

International Journal of Science and Research Archive, 2024, 13(01), 2296–2319

Publication history: Received on 02 September 2024; revised on 10 October 2024; accepted on 12 October 2024

Article DOI: https://doi.org/10.30574/ijsra.2024.13.1.1922

Abstract

The study of geoelectrical resistivity provides critical insights into subsurface characteristics and aquifer dynamics, particularly in regions with varying geological formations. This research investigates the geoelectrical properties of the aquifer system in Umuahia South, highlighting its significance for sustainable groundwater management. The primary aim of this study is to characterize the geoelectrical layers, assess aquifer thickness and resistivity, and evaluate the implications for groundwater resource management. Vertical Electrical Sounding (VES) was conducted across ten locations to measure the resistivity and thickness of subsurface layers. The data collected were analyzed to identify distinct geoelectrical layers, their respective resistivity values, and thicknesses. The study reveals significant variations in aquifer properties across the region, with VES 1 showcasing the largest thickness of 69.2 m and VES 9 the smallest at 5.2 m. Aquifer thickness decreases from the Benin Formation toward the Ameki and Ogwashi-Asaba Formations. Hydraulic conductivity ranges from 0.207 to 0.954 m/day, indicating varying groundwater flow potential, while transmissivity values vary from 4.965 to 30.441 m^2/day, with 60% of aquifers classified as intermediate. Groundwater Potential Index (GWPI) highlights approximately 70% of the area as high potential, underscoring the need for targeted management strategies to optimize water resource extraction and sustainability. The variability in resistivity and thickness across the study area suggests significant subsurface heterogeneity. High resistivity values indicate favorable conditions for groundwater flow, particularly in areas like VES 6. Conversely, lower resistivity in locations such as VES 9 indicates potential challenges for groundwater storage. This study provides vital information on the aquifer system in Umuahia South, emphasizing the need for targeted groundwater management strategies based on the geoelectrical characteristics identified. The research contributes to a deeper understanding of the aquifer dynamics in the region and offers a framework for sustainable groundwater resource management, highlighting the importance of geoelectrical assessments.

Keywords: Aquifer assessment; Geoelectrical resistivity; Groundwater management; Subsurface heterogeneity

1. Introduction

Groundwater plays a crucial role in the global water cycle, serving as an essential resource for human consumption, agriculture, and delicate ecosystems. In many regions, particularly in sub-Saharan Africa, groundwater is the primary source of freshwater, driving socio-economic development (Chinye-Ikejiunor et al., 2021; Odochi et al., 2024). In the Umuahia South area, however, groundwater resources are facing significant pressures due to rapid urbanization and a

* Corresponding author: Bridget Odochi Ubechu

steadily increasing population. This growing demand underscores the urgent need for comprehensive studies to elucidate the dynamics of groundwater in this region and ensure its sustainable management (Ijioma, 2021).

Understanding the occurrence, movement, and flow direction of groundwater is essential, especially in regions where it exists beneath the surface. Aquifers—subterranean layers of rock, sand, or gravel—contain and transmit water when accessed through boreholes (Opara et al., 2020). The characteristics of these aquifers can vary significantly based on several factors, including geological settings, types of rocks or sediments, and the volume of water stored within them. (Okoli et al., 2024) Key parameters such as hydraulic conductivity, transverse resistance, longitudinal conductance, and transmissivity are vital for assessing the groundwater potential of an area.

Hydraulic conductivity measures how easily water can flow through an aquifer, influenced by the porosity and permeability of the geological materials. High hydraulic conductivity indicates that water can move freely, making such aquifers more accessible for extraction. Conversely, low hydraulic conductivity can hinder water movement, complicating access to this vital resource (Anomohanran et al., 2020). Transverse resistance reflects an aquifer's ability to transmit groundwater laterally, which is important for understanding how water may spread across a region (Eugene-Okorie et al., 2020). Longitudinal conductance, on the other hand, provides insight into vertical groundwater flow, helping to assess how water moves between different aquifer layers (Abdulrazzaq et al., 2020). Transmissivity is another crucial metric that indicates how much water can be transmitted through a unit width of an aquifer under a hydraulic gradient, further aiding in the evaluation of an aquifer's potential (Joshua et al., 2023).

Understanding these parameters is essential for effective groundwater management, especially in urban areas experiencing high demand for water resources (Akaolisa et al., 2022). A comprehensive understanding of groundwater dynamics can facilitate better planning and resource allocation, ensuring that the needs of the population are met without compromising the integrity of the aquifer system. Groundwater serves as a reliable water source during droughts or when surface water resources are limited. In the Umuahia South area, where agriculture is a vital component of the economy, having access to groundwater becomes crucial for crop irrigation and livestock farming (Mgbenu & Egbueri, 2019). By studying the groundwater potential in this region, authorities can identify areas with sufficient groundwater reserves that can be tapped into during dry spells. This proactive approach enhances community resilience to water scarcity, ensuring a consistent supply, even during prolonged dry periods. The identification of suitable locations for boreholes and wells can significantly improve agricultural productivity, ultimately enhancing food security for the local population (Igwe et al., 2020).

From an environmental perspective, understanding groundwater dynamics is essential for effective water resource management and the prevention of over-exploitation. Sustainable extraction practices are necessary to avoid adverse environmental impacts such as land subsidence or saltwater intrusion (Emenike et al., 2018). Over-extraction of groundwater can lead to severe long-term consequences, including the degradation of the aquifer system and reduced water quality. By examining groundwater potential, this study will contribute to the development of sustainable water management strategies, ensuring the long-term availability of this vital resource (Zacchaeus et al., 2020).

This study explores the groundwater potential of the Umuahia South area using electrical resistivity methods to identify groundwater-bearing formations. Groundwater is vital for domestic, agricultural, and industrial needs, making this research essential for informed water supply planning and infrastructure development, particularly amid rapid urban growth, such as the Industrial Technology Village and a proposed World Bank housing estate. The study aims to pinpoint suitable locations for public water supply systems and borehole drilling while promoting sustainable management practices. By mapping aquifers and recording GPS coordinates at each borehole site, this research seeks to enhance socio-economic development, agricultural productivity, and environmental integrity in the region.

2. Research and Geology of the Area

The study area is located in the Eastern Niger Delta, specifically within latitudes 5°26' to 5°34' N and longitudes 7°22' to 7°33' E as shown in Figure 1. This region is characterized by high relative humidity levels exceeding 70% and temperatures ranging from 29°C to 31°C. It falls within the sub-equatorial belt, receiving an average annual rainfall of about 4,000 mm. Umuahia South Local Government Area (LGA) in Abia State, Nigeria, is bordered by Umuahia North to the north and northeast, Isiala Ngwa North to the south, Ikwuano to the east, and is separated from Imo State by the Imo River to the west. Topographically, Umuahia South has a low-lying elevation between 20 and 200 meters above sea level, featuring a network of streams and rivers. The Imo River is critical to the area's drainage system, flowing southward into the Atlantic Ocean. Anya River, a tributary of the Kwa Ibo River, traverses the southeastern part of the area (Uchendu et al., 2019).

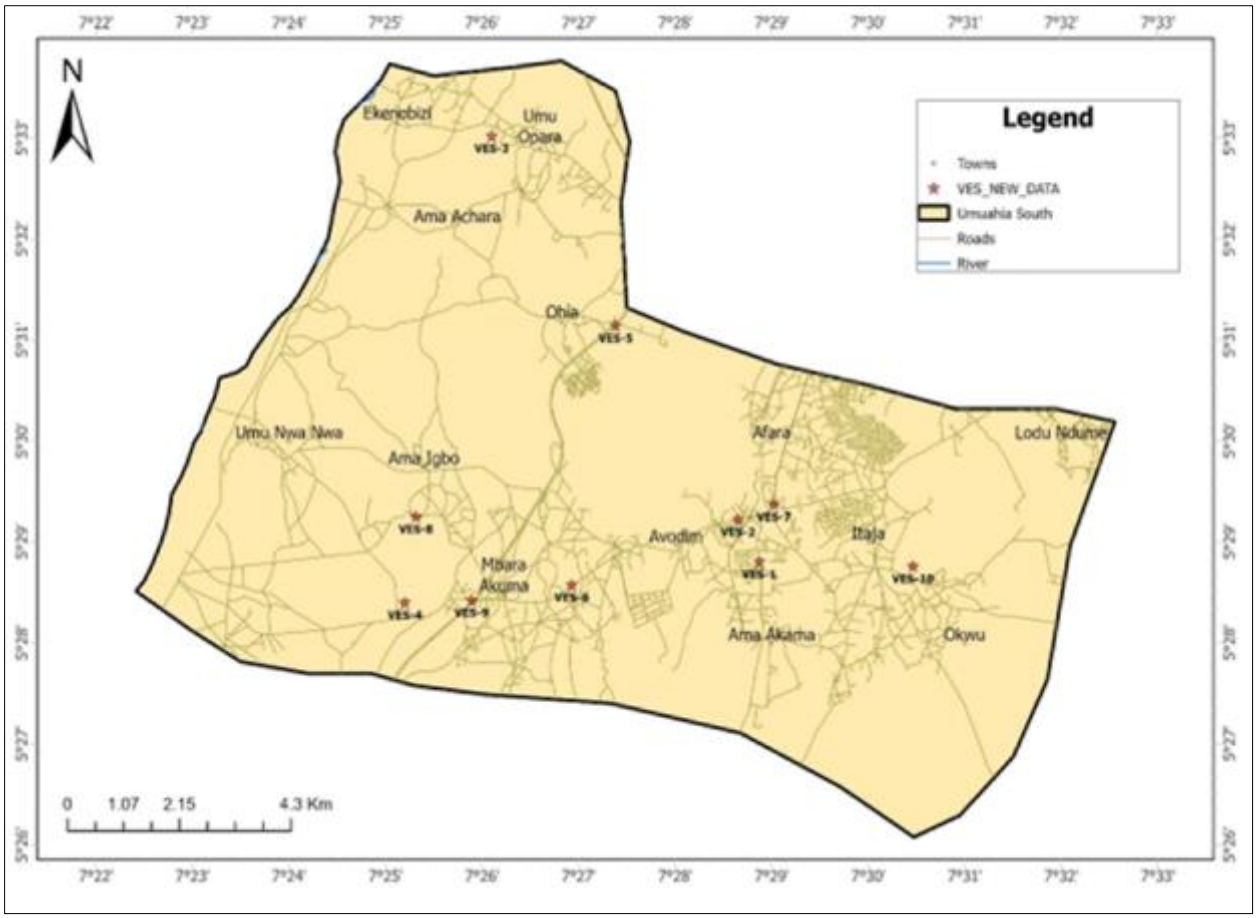

Figure 1 Map of the study area showing the VES Points

The climate in Umuahia South LGA is tropical, with a wet and dry season. The rainy season typically begins in April and lasts until October, with peak rainfall between June and September. The dry season occurs from November to March, with reduced rainfall but occasional isolated showers. The region maintains high humidity year-round, contributing to a muggy climate, especially during the rainy season (Onwuka & Adesemuyi, 2019). This rainforest climate supports diverse vegetation, including various shrub species, tropical forests, grasslands, and agricultural lands. The area's fertile soil is conducive to agricultural activities, making Umuahia South an important region for food production. Understanding the groundwater dynamics in this area is essential for sustainable management and development, given the pressures from urbanization and population growth.

The geology of the study area aligns with the Niger Delta complex, characterized by three lithostratigraphic units: the Marine Akata Formation, Paralic Agbada Formation, and the Continental Benin Formation as shown in Figure 2. These Tertiary sediments reach a thickness of approximately 10,000 meters, with the Akata and Agbada Formations serving as source and reservoir rocks for petroleum. However, all boreholes in the Tertiary Niger Delta utilize water from the Benin Formation, which outcrops in the Umuahia South area (Amos-Uhegbu, 2014).

This area uniquely features the Benin hydrogeological setting in Abia State, comprising Oligocene to Recent Ogwashi-Asaba Formation (upper member) and Miocene to Recent Coastal Plain Sands (lower member) (Reijers, 2011). The Coastal Plain Sands consist of thick, unconsolidated, medium- to coarse-grained, pebbly sands interspersed with lenses of poorly cemented sands and clay, creating multi-aquifer systems separated by aquitards. Petrographic analysis indicates that the rock composition includes 95-99% quartz grains, with minor amounts of mica, feldspar, and dark-colored minerals (Reijers, 2011). The Benin Formation, predominantly present, is about 200 meters thick, characterized by unconsolidated, cross-bedded sands with localized clays and shales, yielding significant water supplies from its aquifers (Agharanya & Dim, 2018).

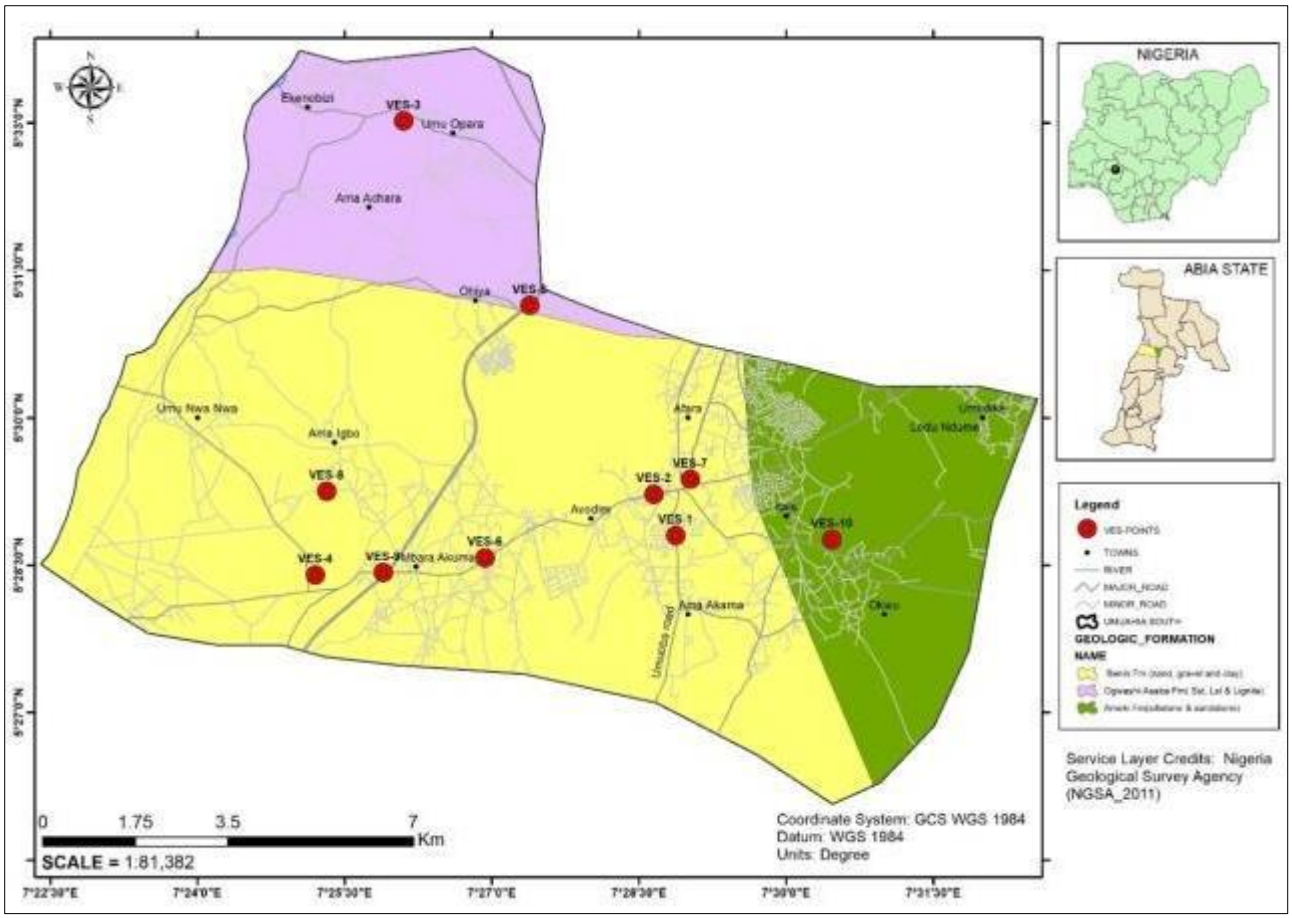

Figure 2 Geologic Map of the Study Area

3. Methodology

3.1. Methods

The research methodology involved a comprehensive literature review and an examination of the study area map. Subsequently, a field survey was conducted to collect data and observations on the geological features of the area, focusing on hydrogeological aspects. This included geo-electrical sounding and interpretation of both surface geological and geo-electrical data.

Resistivity measurements were taken using a Terrameter SAS 4000 system. A combination of computer analysis and visual inspection was employed to identify the VES curves based on the shapes produced from the field data. This process facilitated the inference of the relative magnitudes of different geoelectric layers. The field data were plotted on bi-logarithmic coordinates as sounding curves, illustrating the variations in apparent resistivity as a function of half current electrode spacing. A smooth curve was then drawn through these points to generate the field curves.

3.1.1. Data Acquisition

Various surface geophysical techniques are available for groundwater exploration, but the Electrical Resistivity Method is the most widely used. This method measures the apparent resistivity of the subsurface, aiding in the identification of bedrock fractures, contaminants, and groundwater. Variations in electrical resistivity can indicate changes in rock composition, layer thickness of the weathered zone, or overburden (Fajana, 2020). The resistivity of subsurface materials, such as rocks and minerals, is influenced by factors like lithology, porosity, water saturation, and the presence of voids in the rocks. Soil electrical resistivity reflects the soil's ability to conduct electrical current and serves as a key indicator of permeability, helping to predict its water-bearing capacity (Ibuot et al., 2022).

In this study, the Electrical Resistivity Method was employed using the Schlumberger configuration. A direct current (D.C.) was passed into the soil through a pair of current electrodes, while the potential difference (Δv) resulting from

this current flow was measured using a second pair of electrodes (potential electrodes). Figure 3 provides a schematic representation of the field data acquisition process and subsurface current interactions.

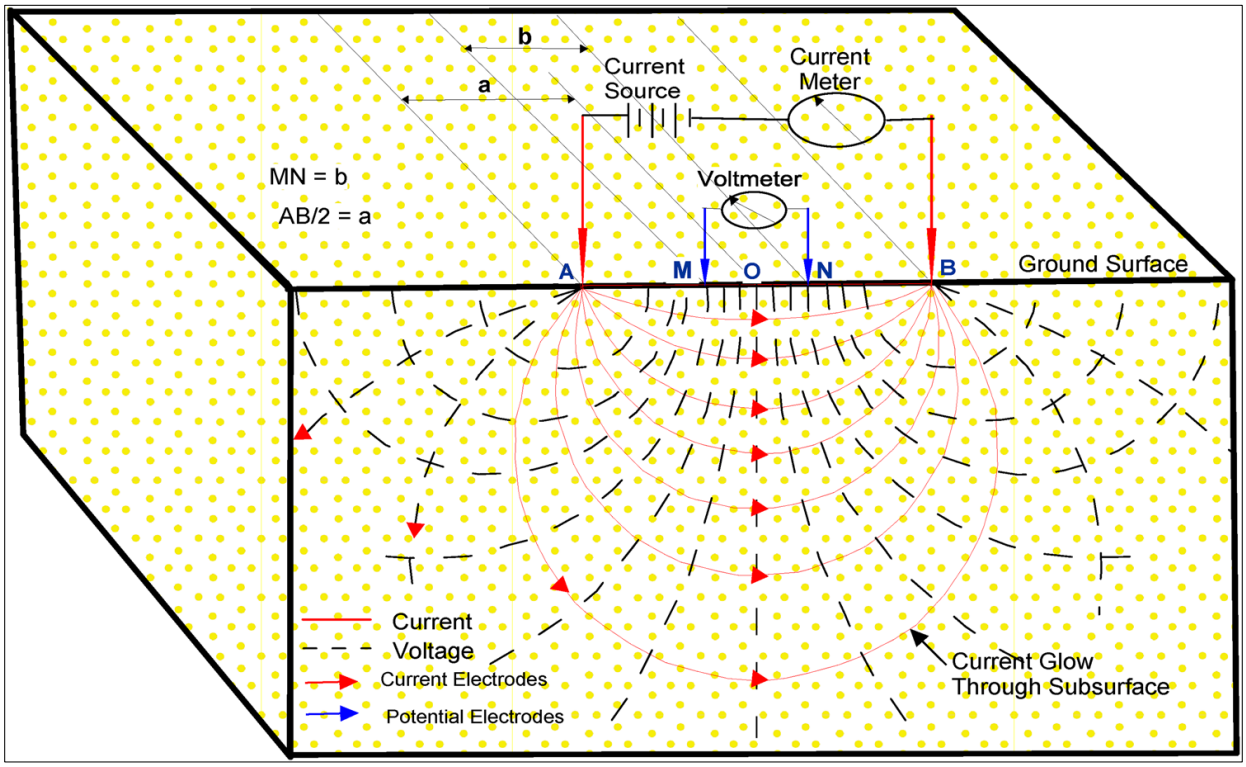

Figure 3 Schematic diagram illustrating the setup for Electrical Resistivity Measurement, adapted from Akiang et al. (2024)

In practice, increasing the spacing between the outer current electrodes allows the electric current to penetrate deeper into the earth, enhancing the depth of investigation. The ground responses depend on rock type, fluid content in pore spaces, and the hydrogeochemical characteristics of the contained fluids (Aleke et al., 2018).

Sounding locations were randomly selected across ten communities (Table 1). A total of ten VES datasets were collected, with a maximum current electrode separation (A-B) of 400 meters and potential electrodes (M-N) set at 20 meters. The four-electrode array technique was employed on the surface, using one pair to input current into the ground and the other pair to measure potential. Using the Schlumberger array, the apparent resistivity (ρ) measured at a specific location can be expressed as:

$$\rho a(s) = R\pi \left(\frac{a^2}{b} - \frac{b}{4}\right) \quad \text{.....1}$$

Where: a = difference between the spacing of the current electrodes and half the electrode distance (AB), b = ratio of the potential electrode spacing to the potential electrode distance (MN) The resistance R can be calculated using the relationship between the current I and voltage V.

$$R = \frac{V}{I} \quad \text{..... 2}$$

Equation (2) can be written as:

$$\rho a(s) = K \times R \quad \text{..... 3}$$

Geometric Factor

$$K = \pi \left(\frac{a^2}{b} - \frac{a}{4}\right) \quad \text{..... 4}$$

The spatial arrangement of the electrodes in the ground influences a parameter known as the geometric factor (K), which can be determined for different electrode configurations. The VES method was selected for its ability to provide detailed information about the vertical succession of thickness and resistivity, allowing for the delineation of subsurface stratigraphy based on resistivity variations.

Table 1 Locations for VES Soundings

VES No	Name of Location	Latitude (°N)	Longitude (°E)	Elevation (m)
1	Umuelem Amakama	5°28'31.27''	7°29'02.01''	153
2	Old Umuahia	5°13'00.16''	7°30'00.27''	152
3	Ekenobizi	5°29'16.07''	7°28'58.33''	151
4	Ohiocha	5°26'16.23''	7°26'58.09''	114
5	Ohiya	5°57'00.01''	7°23'00.11''	174
6	Nsirimo	5°33'00.03''	7°25'00.18''	122
7	Umuobia-isi Court	5°23'06.08''	7°34'37.05''	132
8	Umunwanwa	5°30'38.11''	7°24'01.08''	155
9	Mgbarakuma	5°30'54.22''	7°27'21.02''	120
10	Itaja	5°28'09.06''	7°23'02.13''	152

3.2. Data Processing

3.2.1. Vertical Electrical Sounding

The data from VES is plotted as a graph of apparent resistivity versus half current electrode spacing on a log-log scale using Microsoft Excel. The inflection point on the graph indicates the depth to the interface, approximated as two-thirds (2/3) of the electrode spacing at that point. This approximation aids in computer iterative modeling. The apparent resistivity is plotted on the ordinate against half current electrode spacing to generate the sounding curve on bi-logarithmic paper. Geo-electric layer parameters, such as apparent resistivity, depth, and thickness, are derived from asymptotic methods and used as input data for computer modeling (Abraham et al., 2018).

The VES data were processed using the 1-D WINRESIST™ software to determine layer parameters. Iterations between 1 and 29 minimized errors and enhanced the goodness-of-fit. This procedure yielded true resistivity layers, along with their corresponding thicknesses and depths, which were utilized as Dar-Zarrouk parameters.

3.2.2. Longitudinal Conductance and Transverse Resistance Estimation

Longitudinal conductance (S_L) provides an indication of a layer's impermeability and is crucial in identifying groundwater potential targets. High S_L values suggest the presence of relatively thick, protective layers that shield the aquifer. These layers act as a protective cover, making them important for groundwater potential assessments (Nwachukwu et al., 2019). Table 2 presents the classification of protective layers based on calculated SL values, where high SL indicates priority for groundwater potential. The following equations are used to calculate longitudinal conductance:

$$H = \sum_{i=1}^{h} hi \qquad \ldots\ldots\ldots\ldots \qquad 5$$

$$S_L = \frac{h1}{\rho 1} + \frac{h2}{\rho 2} + \frac{h3}{\rho 3} + \frac{h4}{\rho 4} \ldots \frac{hn}{\rho n} = \sum_{i=1}^{n} \frac{hi}{\rho i \rho} \quad \ldots\ldots\ldots\ldots 6$$

where: ρ represents the layer resistivity in Ωm, h is the layer thickness in meters (m), S_L is the longitudinal conductance in mhos.

Table 2 Protective Capacity Rating

Longitudinal Conductance (S_L)	**Protective Capacity**
>10	Excellent
5 - 10	Very good
0.7 – 4.9	Good
0.2 – 0.69	Moderate
0.1 – 0.19	Weak
< 0.1	Poor

This parameter helps identify areas with good groundwater potential in the investigation target zone. The transmissivity values of aquiferous zones are determined by the highest transverse resistance (R_T) values. The Dar-Zarrouk parameters for a horizontal, homogeneous, and isotropic layer can be calculated as follows:

$$R_T = \rho_1 h_1 + \rho_2 h_2 + \rho_3 h_3 + \rho_4 h_4 + \cdots \rho_n h_n = \sum_{i=1}^{n} \rho_i h_i \quad \text{.....7}$$

where: ρ is the layer resistivity in Ωm, h is the layer thickness in m, R_T is the transverse resistance in Ωm^2

3.2.3. Hydraulic Conductivity and Aquifer Transmissivity Estimation

Hydraulic conductivity (K) is a crucial parameter for understanding groundwater flow and aquifer potential. In the absence of direct measurements from pumping tests, this study employed alternative methods, such as the Dar Zarrouk parameters and the concept of "real resistivity," to indirectly assess hydraulic conductivity. These methods are effective for determining aquifer properties, including transmissivity and the protective capacity of overlying rock materials (Agbasi et al., 2019; Akiang et al., 2024).

Hydraulic conductivity (K) reflects an aquifer's ability to transport water under a hydraulic gradient, while transmissivity (T) indicates the aquifer's capacity to transmit groundwater through its entire saturated thickness. Areas with high transmissivity values suggest a greater potential for groundwater resources. Hydraulic conductance is directly proportional to layer resistivity and permeability; regions with low resistivity values will exhibit high hydraulic conductivity, facilitating fluid flow and contaminant circulation (Fatoba et al., 2014).

The relationship between aquifer transmissivity (T) and hydraulic conductivity (K) is defined by the following equation:

$$K = 386.40 R_{rw}^{-0.93283} \quad \text{.....} \quad 8$$

In this formula, *Rrw* represents the resistivity of the aquifer (interpreted from the curves). Hydraulic conductivity (K) is calculated using the given equation. Aquifer transmissivity (T, in m^2/day) is then determined by multiplying the hydraulic conductivity by the thickness of the aquifer layer.

$$T = Kh \quad \text{.....} \quad 9$$

Where, K represents the hydraulic conductivity (m/day), and h denotes the layer thickness (m). Table 3 provides the classification of aquifers based on transmissivity values, as outlined by Akiang et al., 2024.

Table 3 Aquifer Classification Based on Transmissivity (Akiang et al., 2024)

Transmissivity (m^2/day)	Aquifer Rating	Groundwater Supply Potential
>1000	Very Good	Suitable for large-scale regional withdrawal
100 - 1000	High	Suitable for moderate regional withdrawal
10 - 100	Intermediate	Local supply for small communities or plants
1 - 10	Low	Small-scale local supply (e.g., private use)
0.1 - 1	Very Low	Limited private water supply
<0.1	Impermeable	Difficult to extract local water supplies

3.2.4. Coefficient of Anisotropy (λ)

The coefficient of anisotropy (λ) reflects the degree of anisotropy in an aquifer system. Higher values of λ indicate materials with low porosity and permeability, while lower values correspond to zones with high aquifer potential (Akinrinade & Adesina, 2016). It is calculated as follows:

$$\lambda = \sqrt{\frac{R_t}{R_s}} \qquad \text{……10}$$

Where: R*t* refers to the transverse resistivity, and the Rs represents the longitudinal resistivity.

3.2.5. Groundwater Potential Index (GWPI)

Key factors influencing groundwater potential include aquifer thickness, aquifer resistivity, the coefficient of anisotropy, transmissivity, and hydraulic conductivity are rated according to Table 4. Each parameter's influence is assigned a weight based on its significance in groundwater dynamics, with a ranking scale of 1 (low), 3 (medium), and 5 (high). GWPI is calculated using equation (11):

$$GWPI = \sum(W_i R_i) \qquad \text{……11}$$

where: W_i = weight of parameter i, R_i = rating score of parameter i

Each parameter's weight (W) is set at 20%. Thus, the GWPI is a function of the coefficient of anisotropy (CA), aquifer thickness (AT), aquifer resistivity (AR), transmissivity (T), and hydraulic conductivity (K). The equation for GWPI is:

$$GWPI = CA_w CA_R + AT_w AT_R + AR_w AR_R + T_w T_R + K_w K_R \qquad \text{……12}$$

The GWPI values for each VES point were imported into an ArcGIS environment, and the Inverse Distance Weighting (IDW) tool was used to create the groundwater potential map.

Table 4 Groundwater Potential Rating

Groundwater Potential Factor	Categories/Classes	Potential Rating	Ratings	Weight (%)
Coefficient of anisotropy (CA)	<1	Low	1	20
	1-1.5	Medium	3	
	1.5-1.9	High	5	
Aquifer thickness (AT)	2-10	Low	1	20
	10-20	Medium	3	
	>20	High	5	
Aquifer resistivity (AR)	10-40	Low	1	20
	40-100	Medium	3	
	100-300	High	5	
Transmissivity (T)	1-10	Low	1	20
	10-100	Medium	3	
	100-1000	High	5	
Hydraulic Conductivity (K)	$10^{-3} – 10^{-5}$	Low	1	20
	$10^{-1} – 10^{-3}$	Medium	3	
	$>10^{-1}$	High	5	

4. Result and Discussion

4.1. Geoelectrical Layers Characteristics

The study area is primarily composed of sand interspersed with clay from the Benin Formation. The groundwater potential within this formation is largely influenced by the thickness of the sandy layers. A total of ten VES were conducted in Umuahia South to assess groundwater occurrence, with the summarized results presented in Table 5. The VES models generated using WINRESIST software are illustrated in Figure 4.

Table 5 highlights that the study area consists of four distinct geo-electrical layers. The resistivity of the first layer (topsoil) ranges from 2.4 to 191.9 Ω m, with an average value of 157.68 Ω m. The thickness of this first layer varies from 1.2 to 8.8 m, yielding a mean thickness of 3.72 m. The second layer, identified as clayey sand and sandy clay, exhibits a resistivity range of 64.4 to 281.4 Ω m, with a mean value of 129.7 Ω m. Its thickness varies between 3.7 and 11.3 m, resulting in an average thickness of 6.05 m. The third layer displays a resistivity range from 624.3 to 3,209.1 Ω m, averaging 2,052.01 Ω m, while its thickness ranges from 5.2 to 69.2 m. This aquifer system predominantly exists within the third and fourth layers, characterized mainly by sandstone, except for VES 2, which contains sandy clay. The resistivity values for the fourth layer range from 53.4 to 1,734.3 Ω m, with an average resistivity of 735.93 Ω m. Due to the maximum current injected by the electrodes being insufficient to fully penetrate this layer, its exact thickness and depth remain undetermined. The significant variation in resistivity values is attributed to inhomogeneities within the subsurface layers.

Table 5 Geoelectrical Resistivity and Layer Thickness Results from VES

VES	Locations	ρ_1 (Ωm)	ρ_2 (Ωm)	ρ_3 (Ωm)	ρ_4 (Ωm)	h_1 (m)	h_2 (m)	h_3 (m)	d_1 (m)	d_2 (m)	d_3 (m)	Curve Type
1	Umuelem Amakama	153.60	92.60	1655.00	53.40	2.10	7.70	69.20	2.10	9.80	79.00	HK
2	Old Umuahia	175.30	76.10	1324.90	149.40	1.50	11.30	64.40	1.50	12.70	77.10	HK
3	Ekenobizi	162.80	64.40	1158.00	739.80	1.50	4.50	12.40	1.50	6.00	18.40	H
4	Ohiocha	182.40	66.30	2910.00	767.00	1.20	5.90	58.00	1.20	7.10	65.10	HK
5	Ohiya	191.90	73.80	1865.20	1488.90	1.50	5.00	64.10	1.50	6.50	70.60	H
6	Nsirimo	112.50	281.40	3209.10	627.00	8.60	5.20	44.10	8.60	13.80	57.90	K
7	Umuobia-isi court	131.40	275.10	3181.70	353.20	8.80	4.90	62.10	8.80	13.80	75.80	K
8	Umunwanwa	157.80	77.70	2787.90	248.60	2.50	6.10	54.90	2.50	8.60	63.50	HK
9	Mgbarakuma	134.90	210.90	624.30	1734.30	7.70	3.70	5.20	7.70	11.40	16.60	H
10	Itaja	174.20	78.70	1804.00	1197.70	1.80	6.20	24.00	1.80	8.00	32.00	H

The results of the ten VES conducted across the study area reveal the presence of four distinct layers. The resistivity distribution of these subsurface layers can be categorized into two main curve types based on their shapes: K-type (where $\rho1 < \rho2 > \rho3$) and H-type (where $\rho1 > \rho2 < \rho3$). The different curve types identified in the study area, as detailed in Table 5, include HK, K, and H. The diversity in curve types further confirms the heterogeneity of the subsurface lithological units in the region.

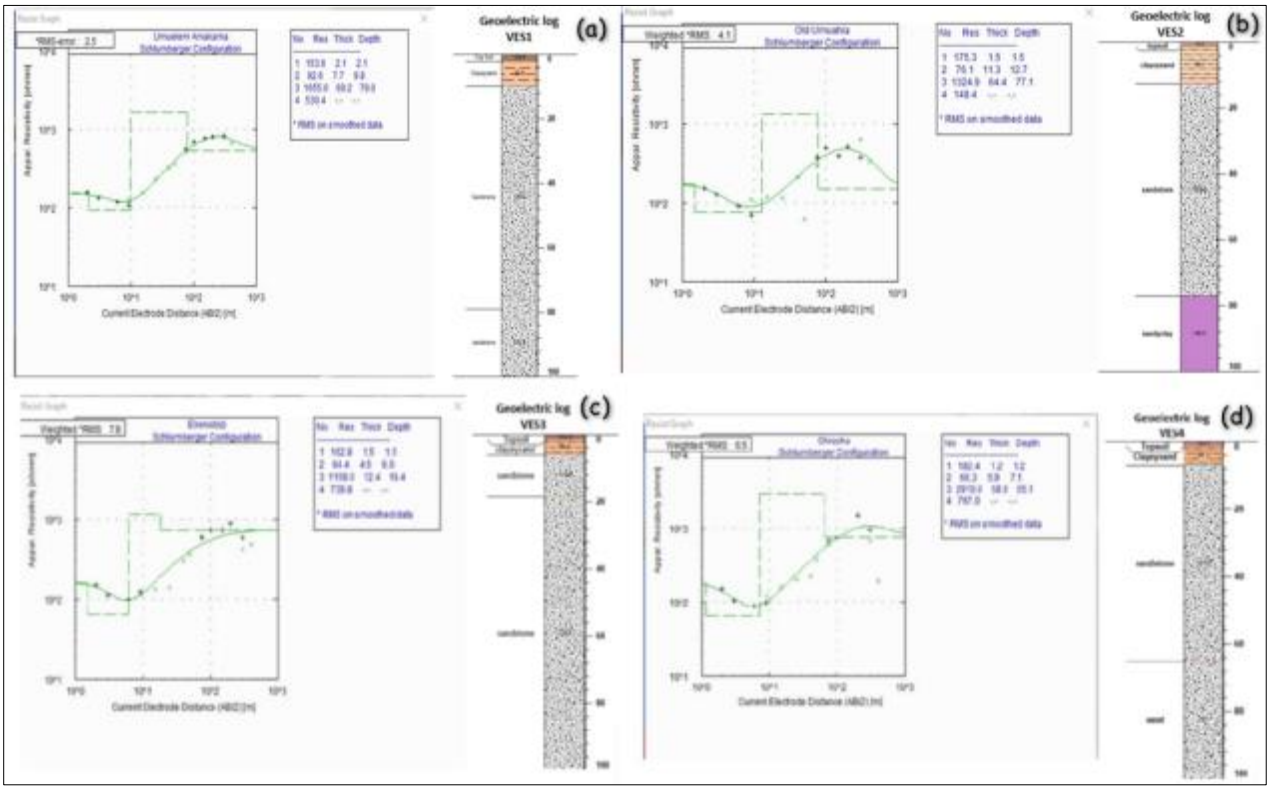

Figure 4 VES Models Obtained from Inversion of Apparent Resistivity Data

The geo-electric correlation sections (Figure 5) and other aquifer parameters (Table 5) reveal both vertical and lateral variations in layer resistivity and thickness, indicating significant lithological changes within the study area. Nearly all the VES points feature sandstone in the third and fourth layers, except for VES 2, which contains sandy clay in the fourth layer. This indicates that the depth to groundwater occurrence in the area ranges from 30 to 80 meters. All VES points exhibit litho-units with textural characteristics that promote groundwater accumulation and discharge. The aquifers in the region are predominantly composed of sandstone.

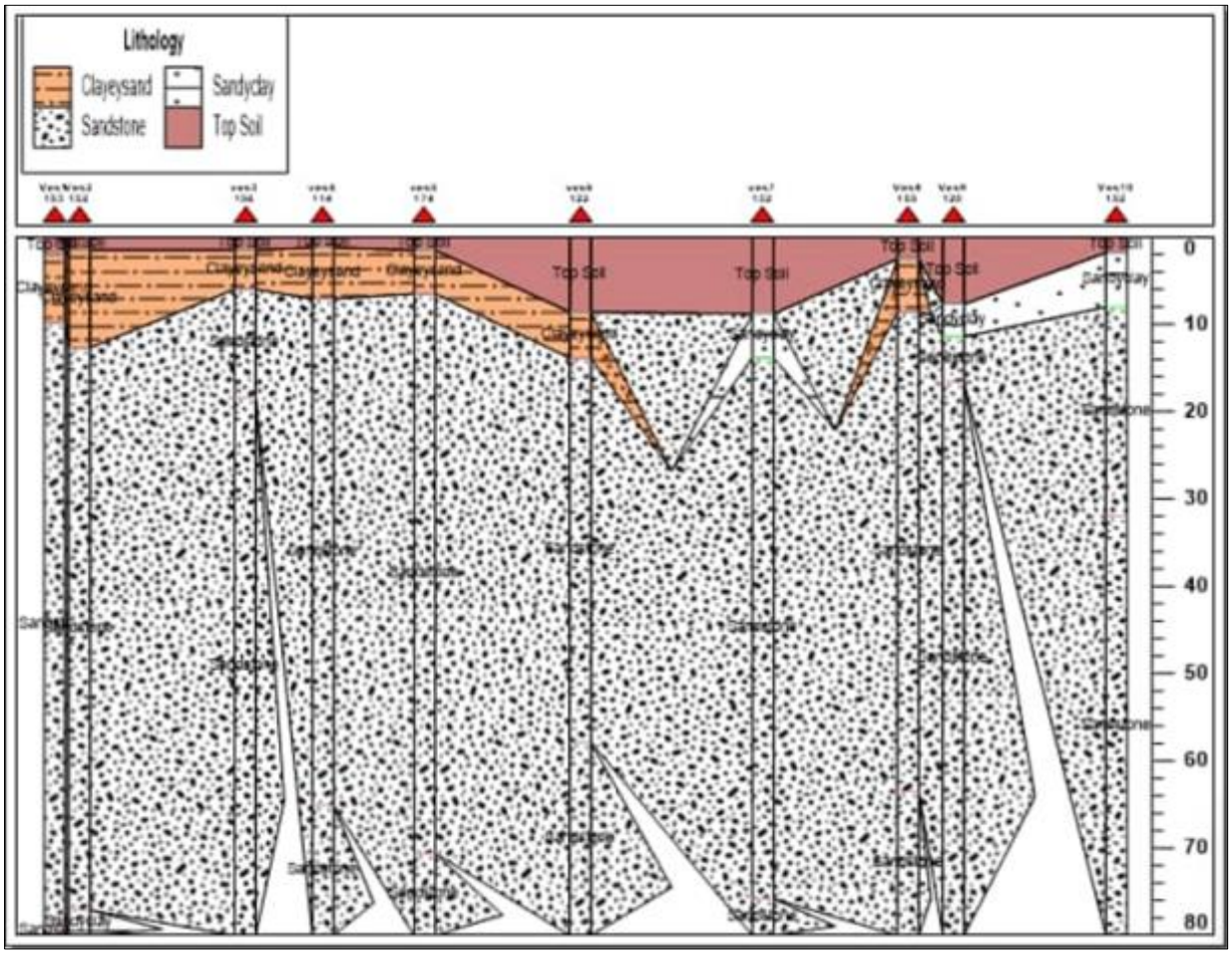

Figure 5 Geo-electric correlation of VES 1 to VES 10

4.2. Aquifer Properties

The results from the VES analysis reveal varying aquifer resistivity, thickness, and depth across the study area, as presented in the Table 6. VES 6 exhibits the highest resistivity of 3209.1 Ωm, while VES 9 shows the lowest at 624.3 Ωm. The thickness of the aquifers ranges from 5.2 m (VES 9) to 69.2 m (VES 1), indicating considerable variability in aquifer properties. The depths to the aquifers vary from 16.6 m (VES 9) to 79.0 m (VES 1), suggesting that groundwater occurrence is accessible at varying depths. The high resistivity values generally indicate the presence of sandstones, which are conducive to groundwater flow (Aleke et al., 2018). However, the lower resistivity at VES 9 may suggest a different lithological composition, such as clay or saturated sands, warranting further investigation to understand the aquifer dynamics better (Ibuot et al., 2019).

Table 6 Summary of Aquifer Characteristics in the Study Area

VES No	Aquifer Resistivity (Ωm)	Aquifer Thickness (m)	Aquifer Depth (m)
1	1655.00	69.20	79.00
2	1324.90	64.40	77.10
3	1158.00	12.40	18.40
4	2910.00	58.00	65.10
5	1865.20	64.10	70.60
6	3209.10	44.10	57.90
7	3181.70	62.10	75.80
8	2787.90	54.90	63.50
9	624.30	5.20	16.60
10	1804.00	24.00	32.00

4.2.1. Aquifer Resistivity

The aquifer resistivity analysis across the study area reveals as shown in Figure 6 and Table 6, notable spatial variability, with resistivity values ranging from 625.587 to 3,208.133 Ωm. Areas with low resistivity, such as Old Umuahia (VES 2), Ekenobizi (VES 3), and Mgbarakuma (VES 9), suggest the presence of less permeable materials, which may hinder groundwater storage. In contrast, Nsirimo (VES 6) exhibits the highest resistivity, indicating a denser aquifer material, while Umuobia (VES 7), Umunwanwa (VES 8), and Ohiocha (VES 4) also present favorable conditions for groundwater accumulation. The largest area, 62.23 sq km, falls within the resistivity range of 1,830.776 - 2,124.476 Ωm, reflecting optimal groundwater storage potential. Conversely, the smallest area, 9.98 sq km, corresponds to resistivity values of 625.587 - 1,486.435 Ωm.

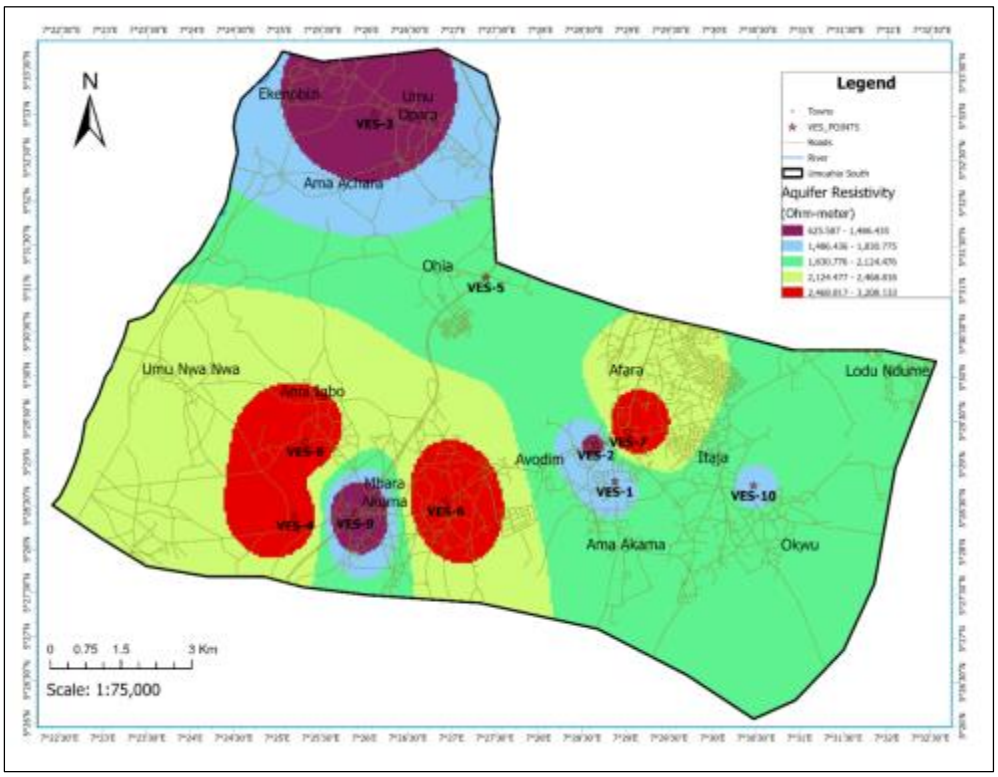

Figure 6 Map Showing Aquifer Resistivity Distribution in the Study Area

4.2.2. Aquifer Thickness

The analysis of aquifer thickness in the study area reveals significant variations as shown in Figure 7 and Table 6, with VES 9 exhibiting the smallest thickness of 5.2 m, while VES 1 presents the largest thickness of 69.2 m. There is a notable decrease in aquifer thickness moving from the Benin Formation toward the Ameki and Ogwashi-Asaba Formations in the northwest and southeast, respectively. The thickness ranges correspond to varying spatial extents: 5.23 to 24.041 m covers 8.22 sq km, while 24.042 to 35.329 m encompasses 14.71 sq km. The range of 35.33 to 43.857 m occupies 25.90 sq km, indicating moderately thick aquifers. The most extensive area, 60.55 sq km, corresponds to thicknesses of 43.858 to 52.636 m, while the deepest aquifer range of 52.637 to 69.191 m accounts for 31.04 sq km. Greater aquifer thickness contributes to higher groundwater storage and enhances protection against external contamination (Eugene-Okorie et al., 2020).

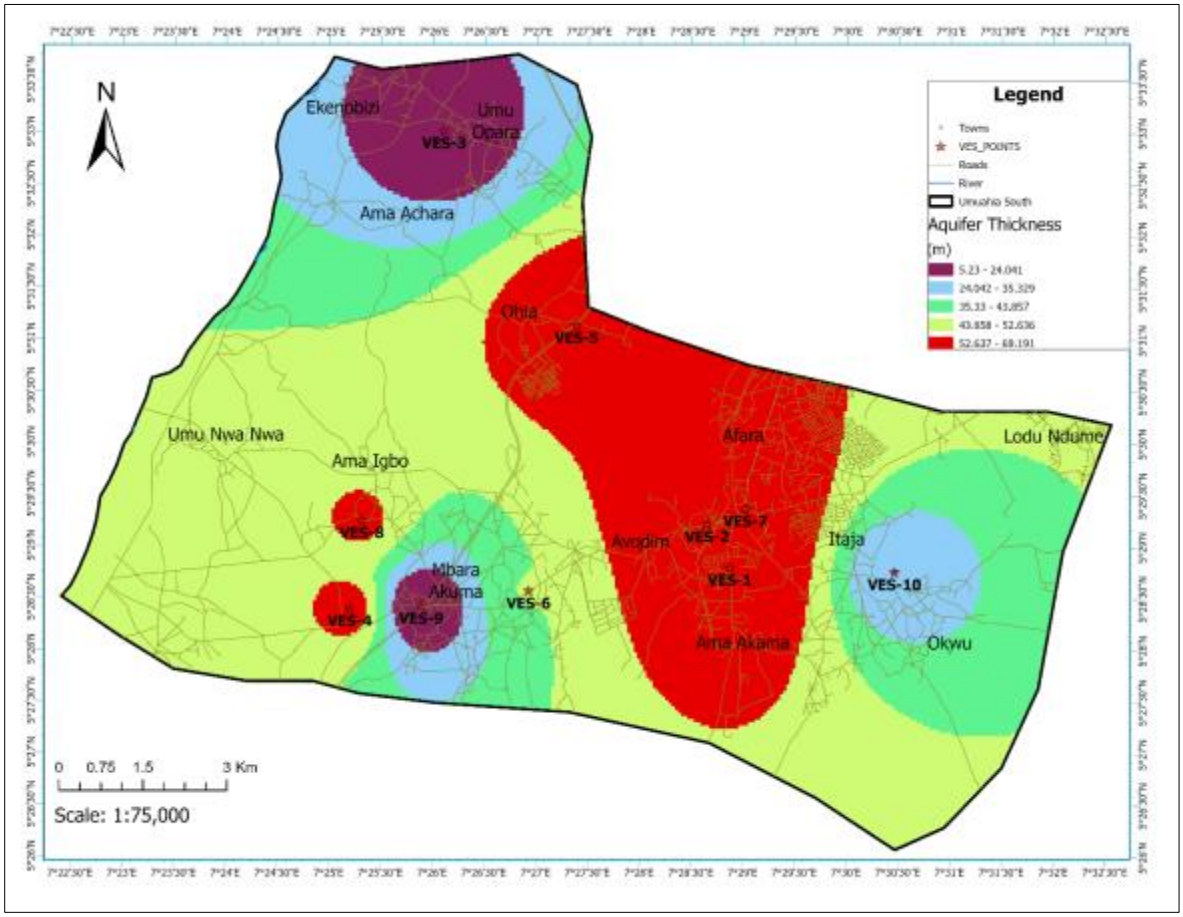

Figure 7 Aquifer Thickness Map of the Study Area

4.2.3. Aquifer Depth

The spatial distribution of aquifer shown in Figure 8 depths ranges from 16.6 m (VES 9) to 79 m (VES 1), indicating the likelihood of deep aquifers in the region and a low risk of borehole failure due to seasonal water table fluctuations (Ejepu et al., 2024). High to moderate aquifer yields are anticipated from VES points 1, 2, 4, 5, 7, and 8, based on their thickness. The spatial distribution map (Figure 8) effectively visualizes areas of varying aquifer depths. The most extensive area, covering 62.882 km^2, corresponds to aquifer depths between 53.07 m and 62.607 m, suggesting substantial groundwater availability. The depth range of 43.776 m to 53.069 m encompasses 24.097 km^2, while shallower (16.628 m to 31.791 m) and deeper ranges (62.608 m to 78.994 m) account for 8.348 km^2 and 31.376 km^2, respectively.

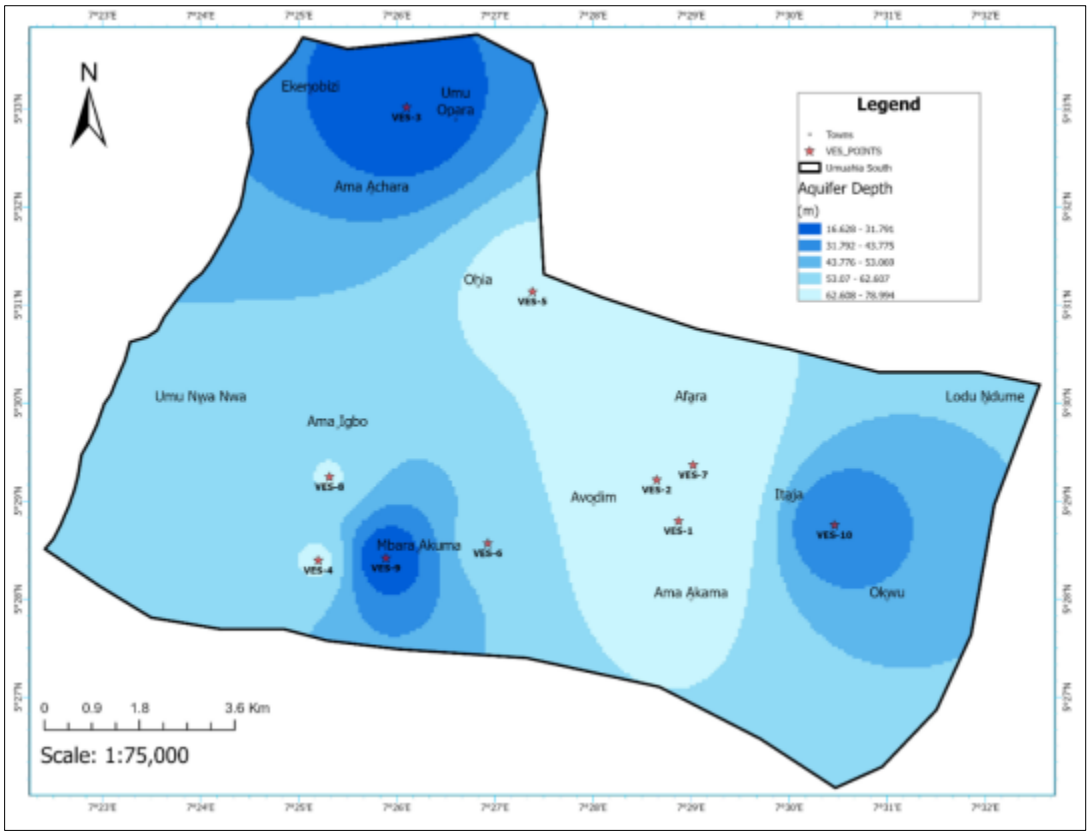

Figure 8 Aquifer Dept Map of the Study Area

4.3. Aquifer Hydraulic Parameters

The Dar-Zarrouk parameters indicate significant variations in aquifer properties across the study area, as shown in Table 7. These differences highlight the diverse hydraulic characteristics of each VES points, which are crucial for understanding groundwater availability and implementing effective management strategies.

Table 7 Dar-Zarrouk Parameters for Aquifers in the Study Area

VES No	Name Of Location	Transverse Resistance (Ωm²)	Longitudinal Conductance (Ω⁻¹)	Hydraulic Conductivity (m/day)	Transmissivity (m²/day)
1	Umuelem Amakama	114,526.00	0.041	0.384	26.579
2	Old Umuahia	85,323.56	0.048	0.473	30.441
3	Ekenobizi	14,359.20	0.011	0.536	6.646
4	Ohiocha	168,780.00	0.020	0.227	13.159
5	Ohiya	119,559.32	0.034	0.344	22.022
6	Nsirimo	141,521.31	0.014	0.207	9.133
7	Umuobia-isi court	197,583.57	0.020	0.209	12.964
8	Umunwanwa	153,055.71	0.020	0.236	12.964
9	Mgbarakuma	3,246.36	0.008	0.954	4.959
10	Itaja	43,296.00	0.013	0.354	8.506

4.3.1. Longitudinal Conductance

Longitudinal conductance measures the ease of groundwater flow parallel to the direction of electric current, reflecting both the impermeability of layers and the horizontal movement of water within aquifers (Nwachukwu et al., 2019). The computed longitudinal conductance values across the study area (Table 7) reveal generally weak conductance, suggesting restricted groundwater flow due to the presence of less permeable materials or discontinuous aquifer formations. Despite this, the aquifer units are characterized by low clay volumes combined with high conductivity and permeability (Ifeanyichukwu et al., 2021).

Locations VES 1 and VES 2, situated within the Benin Formation, exhibit the highest computed longitudinal conductance values, as illustrated in Figure 9. Specifically, the area with conductance between 0.009 and 0.017 Ω^{-1} spans approximately 20.08 sq km, indicating limited flow potential. Conversely, a larger area of 57.90 sq km shows conductance values between 0.018 and 0.022 Ω^{-1}, suggesting moderate aquifer recharge capacity. Additional segments, such as the 31.86 sq km region with conductance from 0.023 to 0.027 Ω^{-1} and the 24.74 sq km area with conductance values of 0.028 to 0.034 Ω^{-1}, enhance the overall groundwater potential. The smallest area, at 5.83 sq km, corresponds to the highest conductance range of 0.035 to 0.049 Ω^{-1}, indicating optimal conditions for groundwater transmission.

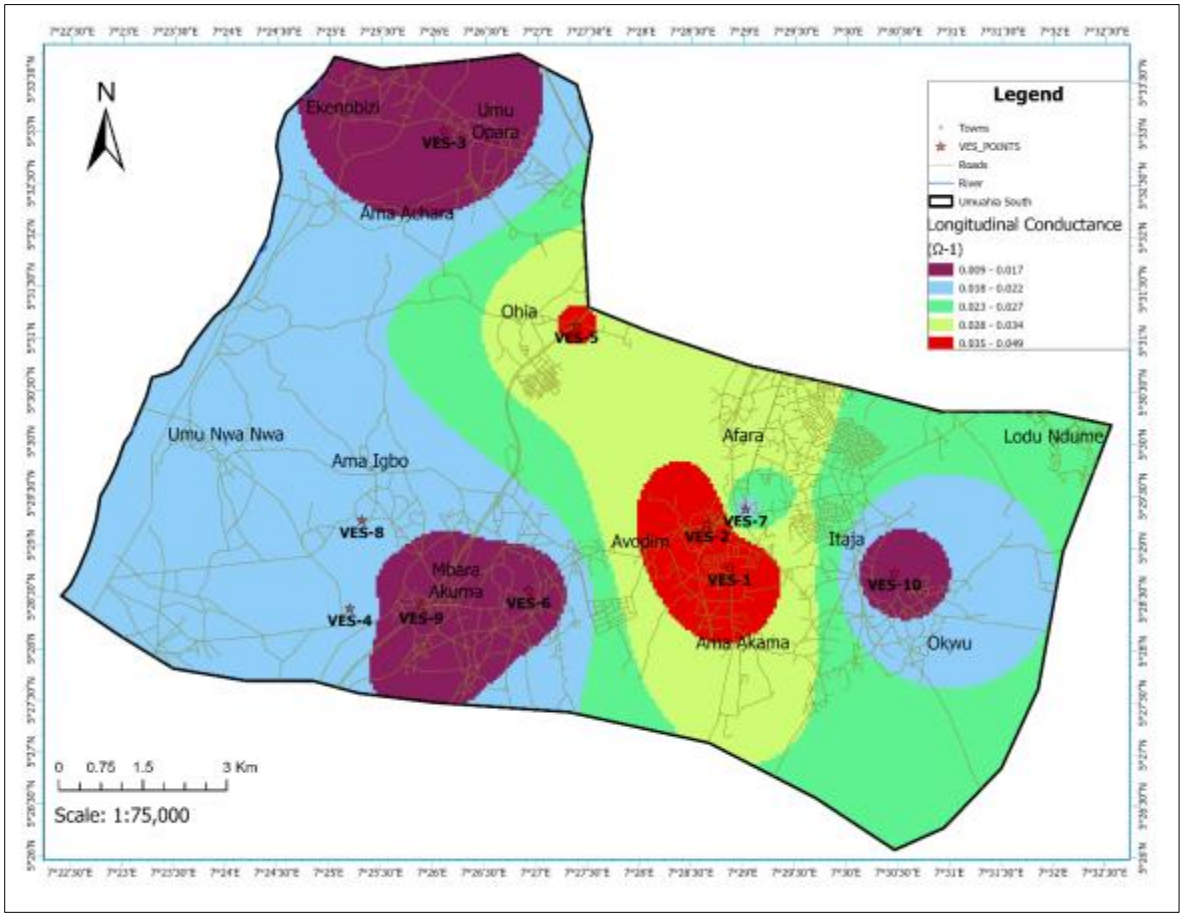

Figure 9 Longitudinal Conductance Map of the Study Area

4.3.2. Aquifer Transverse Resistance

Transverse resistance is a crucial parameter that measures the resistance encountered by groundwater as it flows through an aquifer, perpendicular to the hydraulic gradient. It is calculated as the product of the apparent resistivity of the aquifer layer and its corresponding thickness (Opara et al., 2023). The analysis of transverse resistance values (Table 7) and the accompanying spatial map (Figure 10) reveals a distinct hierarchy in the order of aquifer transverse resistance: VES9 < VES3 < VES10 < VES2 < VES1 < VES5 < VES6 < VES8 < VES4 < VES7.

A high transverse resistance value, such as that seen in VES 4, indicates an aquifer with well-defined limits and limited capacity for lateral water flow. In this scenario, groundwater is effectively channeled and retained within the aquifer, enhancing its overall water-holding capacity, which suggests favorable groundwater potential for the area (Oli et al.,

2020). Conversely, the lower transverse resistance observed in VES 9 suggests a leaky aquifer with poorly defined boundaries. This condition makes it susceptible to pollutants that can infiltrate from adjacent areas, posing a risk to groundwater quality and emphasizing the need for effective aquifer conservation measures (Chinye-Ikejiunor et al., 2021).

The spatial distribution of transverse resistance highlights significant variations across the study area. The most extensive area, covering 63.96 sq km, falls within the resistance range of 105,274.11 to 128,096.579 Ωm, indicating a strong potential for groundwater storage and flow. Following this, the 80,169.395 to 105,274.11 Ωm range covers 33.60 sq km, suggesting moderate aquifer productivity. In contrast, the range of 3,333.749 to 50,500.184 Ωm shows the smallest area at 10.27 sq km, indicating limited groundwater resources.

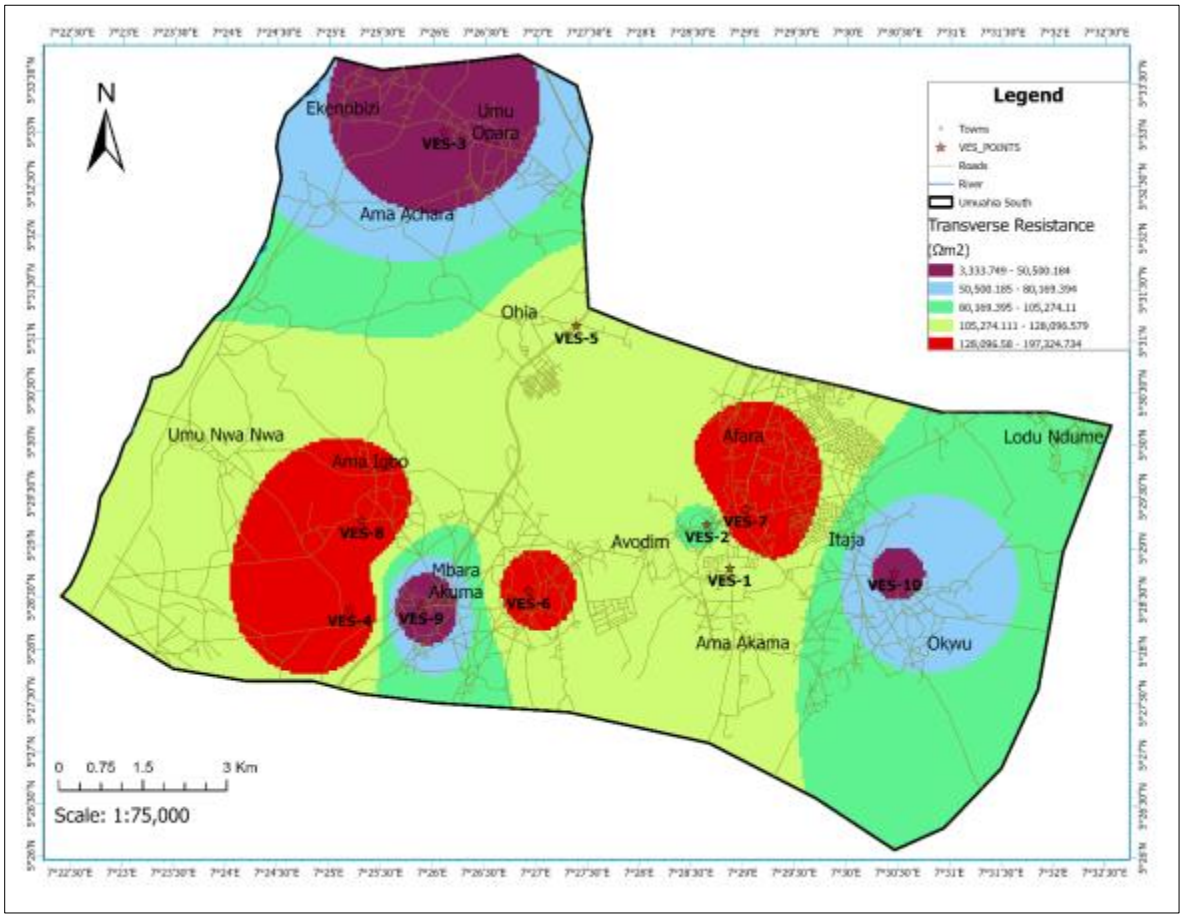

Figure 10 Transverse Resistance Map of the Study Area

4.3.3. Hydraulic Conductivity of the Aquifer

Hydraulic conductivity is a key parameter in understanding the ability of aquifer materials to transmit water, influencing both aquifer productivity and groundwater extraction potential. High hydraulic conductivity values indicate well-connected materials with increased permeability, promoting effective groundwater movement and higher water yields. Conversely, poorly connected aquifer materials result in reduced groundwater flow and, consequently, lower yields (Opara et al., 2020). In the study area, hydraulic conductivity values range from 0.207 m/day (VES 6) to 0.954 m/day (VES 9), with a mean value of 0.392 m/day. This variation reflects different permeability characteristics across the area.

The hydraulic conductivity analysis shows significant spatial variation, with the largest area, 104.15 sq km, exhibiting moderate conductivity (0.331 - 0.421 m/day), suitable for effective groundwater flow. In contrast, only 1.13 sq km corresponds to the highest conductivity range (0.72 - 0.953 m/day), indicating very high permeability and potential for greater water extraction. Lower conductivity values (0.208 - 0.33 m/day) cover 11.82 sq km, while the range of 0.422 - 0.547 m/day encompasses 21.21 sq km. A total of 141.17 sq km of the study area shows favorable conditions for

groundwater recharge. The conductivity increases towards the southwestern region (VES 9), which suggests that targeted groundwater management strategies should focus on these high-yield zones for sustainable water extraction.

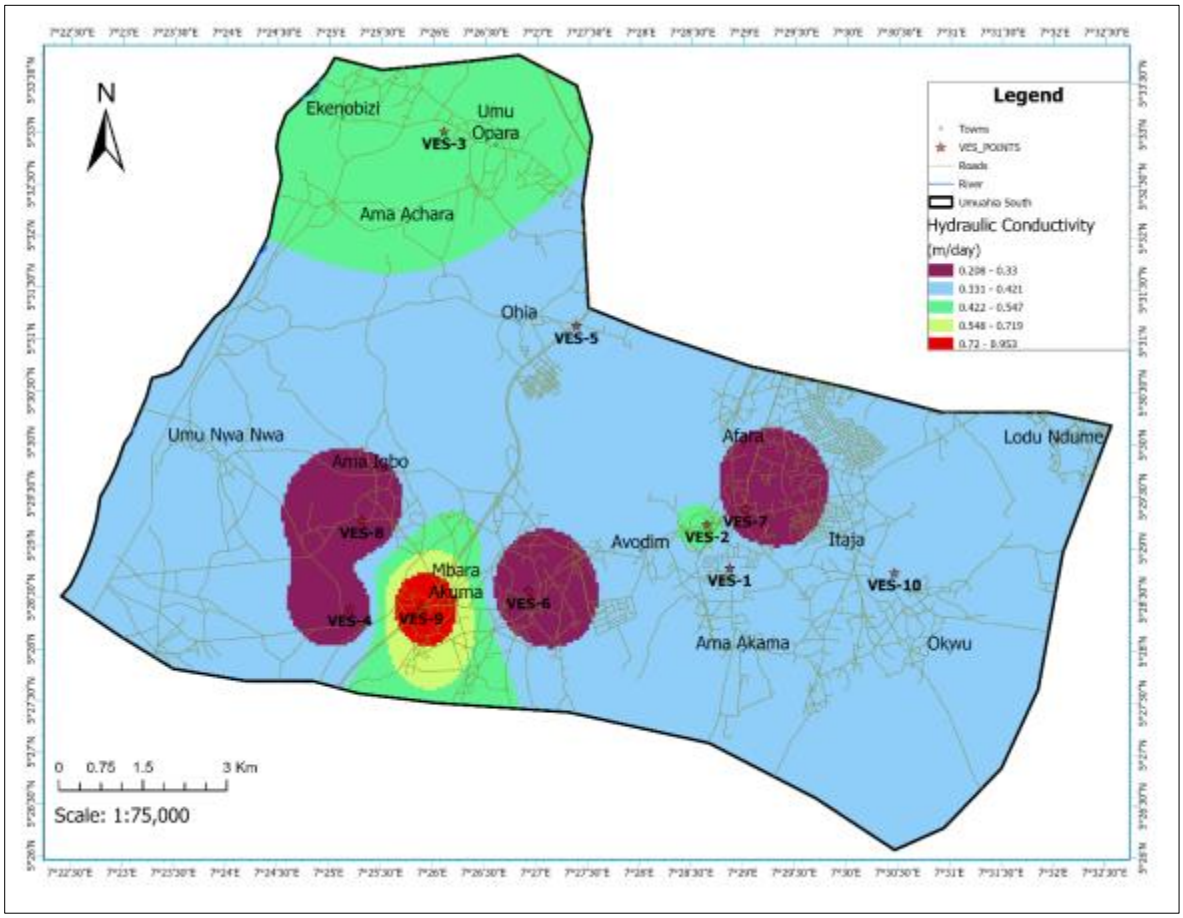

Figure 11 Map of Hydraulic Conductivity of the Study Area

4.3.4. Aquifer transmissivity

Transmissivity measures the speed at which groundwater moves through the saturated zone and the volume of water that can flow through a unit width under specific hydraulic gradient conditions. High transmissivity values indicate a permeable aquifer with elevated hydraulic conductivity (Anosike et al., 2019). In this study, transmissivity values ranged from 4.965 m^2/day to 30.441 m^2/day, with an average of 14.738 m^2/day (Table 7).

The analysis reveals significant spatial variability in transmissivity, highlighting distinct groundwater flow characteristics. The lowest transmissivity range (4.965 - 10.851 m^2/day) covers an area of 20.42 sq km, indicating limited groundwater movement. Conversely, the highest range (21.229 - 30.408 m^2/day) is confined to 7.04 sq km, suggesting enhanced aquifer potential. The intermediate ranges, particularly 10.852 - 14.044 m^2/day (57.68 sq km) and 14.045 - 17.137 m^2/day (30.08 sq km), encompass the largest areas, indicating favorable conditions for groundwater extraction.

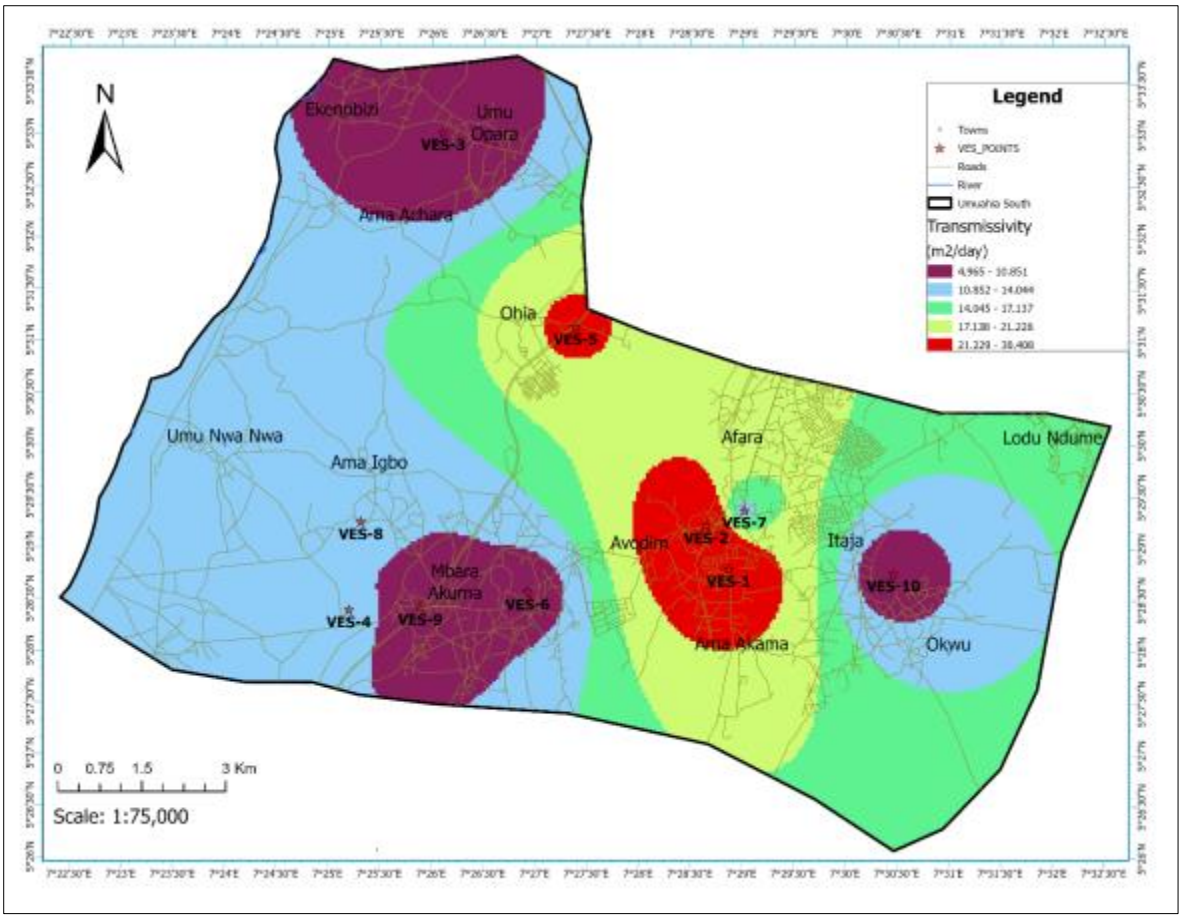

Figure 12 Map of the Aquifer Transmissivity of the Study Area

Figures 12 and Table 8 present the spatial variability of the transmissivity data and its categorization. Results show that approximately 60% of the aquifers in the study area are classified as having intermediate ratings, making them suitable for local water supply for small communities and plants, specifically at VES locations 1, 2, 4, 5, 7, and 8. In contrast, the remaining 40% fall within the low aquifer rating category, signifying withdrawal potential primarily for private consumption at VES locations 3, 6, 9, and 10.

Table 8 Classification of Transmissivity Magnitude in the Study Area Based on Standard

VES No	Aquifer Rating	Groundwater Supply Potential
1	Intermediate	Withdrawal of local water supply (small community, plants etc.)
2	Intermediate	Withdrawal of local water supply (small community, plants etc.)
3	Low	Smaller withdrawal for local water supply (private consumption)
4	Intermediate	Withdrawal of local water supply (small community, plants etc.)
5	Intermediate	Withdrawal of local water supply (small community, plants etc.)
6	Low	Smaller withdrawal for local water supply (private consumption)
7	Intermediate	Withdrawal of local water supply (small community, plants etc.)
8	Intermediate	Withdrawal of local water supply (small community, plants etc.)
9	Low	Smaller withdrawal for local water supply (private consumption)
10	Low	Smaller withdrawal for local water supply (private consumption)

4.3.5. Coefficient of Anisotropy (COA)

Anisotropy is directly related to the hardness of rocks, resulting from their compaction. Consequently, aquifer areas with a high coefficient of anisotropy (COA) tend to have low porosity, typically exhibiting values below one (1), and demonstrate high groundwater potential (George et al., 2020). In contrast, the spatial COA map indicates that VES locations 10, 9, and 3 show low COA values, suggesting high porosity and, consequently, low groundwater potential (Olayinka & Oyedele, 2019). The calculated COA results further reveal that the study areas fall within a sedimentary basin, as all recorded values are less than 1, indicating that the groundwater potential at most VES points in the area is above average.

The analysis of COA across the study area displays significant spatial variation, with specific ranges reflecting differences in subsurface material properties. The range of 0.492 - 0.601 covers an area of 11.21 sq km, indicating relatively isotropic conditions. Meanwhile, the range of 0.602 - 0.666 encompasses 18.86 sq km, suggesting a slight increase in anisotropy. The largest area, 54.09 sq km, falls within the range of 0.667 - 0.721, indicating moderate anisotropy that may influence groundwater flow dynamics. The ranges of 0.722 - 0.779 and 0.780 - 0.87 occupy areas of 24.02 sq km and 32.24 sq km, respectively, reflecting more pronounced directional dependence in these regions.

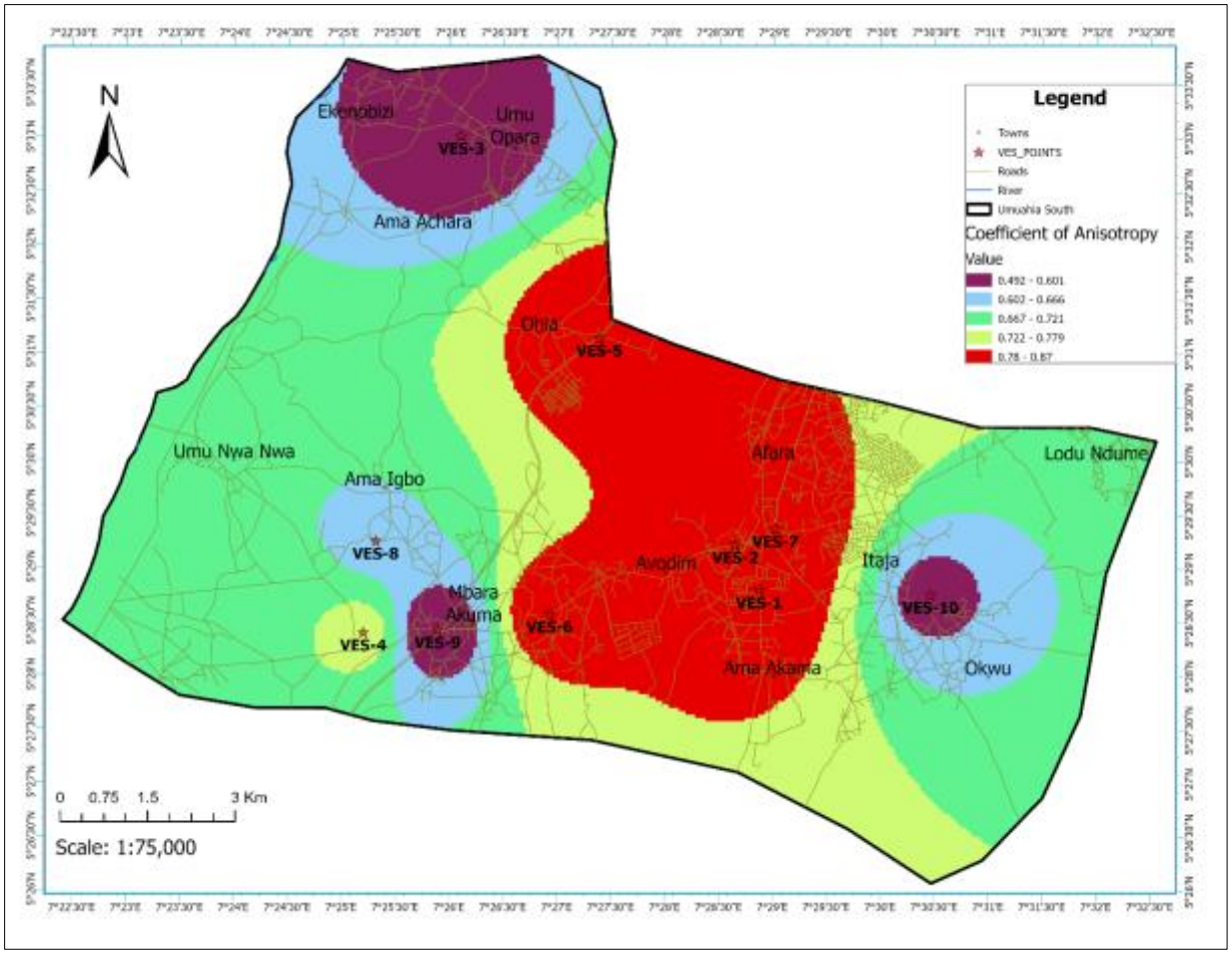

Figure 13 Coefficient of Anisotropy Map of the Study Area

4.4. Assessment of Soil Corrosivity and Protective Capacity

The results presented in Table 9 indicate a uniform assessment of soil corrosivity across all VES locations. Every VES point is classified as "practically noncorrosive," suggesting that the soils in this area have low potential for causing corrosion to buried infrastructure or pipelines. This characteristic is crucial for infrastructure development, as it minimizes the risk of deterioration over time due to soil reactions.

Table 9 Soil Corrosivity and Protective Capacity of VES Locations

VES No	Soil Corrosivity	Protective Capacity
1	Practically noncorrosive	Poor
2	Practically noncorrosive	Poor
3	Practically noncorrosive	Poor
4	Practically noncorrosive	Poor
5	Practically noncorrosive	Poor
6	Practically noncorrosive	Poor
7	Practically noncorrosive	Poor
8	Practically noncorrosive	Poor
9	Practically noncorrosive	Poor
10	Practically noncorrosive	Poor

However, despite the low corrosivity levels, all VES points exhibit a "poor" protective capacity. This indicates a limited ability to shield structures from external corrosive agents, which may compromise the longevity of materials used in construction and installation. The qualitative assessment implies a need for careful consideration in engineering practices, particularly when planning for water or sewage pipelines.

Given the consistent findings across all locations, stakeholders should prioritize monitoring and implementing protective measures to enhance the soil's capacity. Overall, while the low corrosivity is advantageous, addressing the poor protective capacity is vital to safeguard infrastructure investments in the area.

4.5. Assessment of GWPI

GWPI for the study area ranges from 100 to 260, providing the basis for a comprehensive groundwater potential model. This model incorporates various hydrogeological parameters, including aquifer resistivity, thickness, coefficient of anisotropy, hydraulic conductivity, and transmissivity. The resulting classification delineates the study area into two main categories: medium and high groundwater potential zones. Approximately 30% of the area is classified as medium potential, while about 70% falls within high groundwater potential zones, as illustrated in Figure 14. This categorization indicates that the groundwater potential in the study area is generally rated between medium to high.

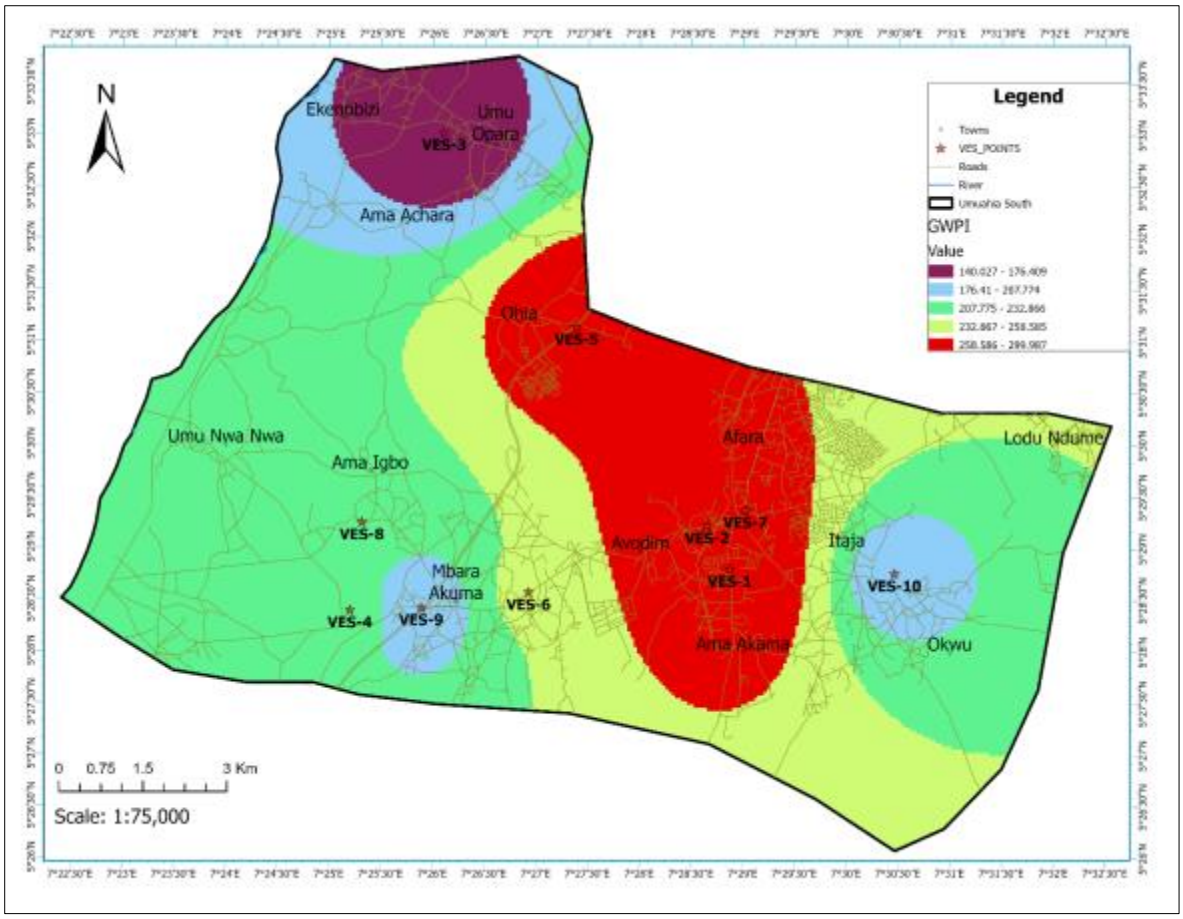

Figure 14 Map of GWPI of the study area

Further analysis reveals significant variations in aquifer potential across the landscape. Areas with GWPI values from 140.027 to 176.409 Ωm span around 7.51 sq km, suggesting limited groundwater availability. In contrast, a larger expanse of 59.25 sq km falls within the GWPI range of 207.775 to 232.866 Ωm, indicating moderate groundwater potential and favorable conditions for aquifer recharge and storage. Meanwhile, regions with GWPI values of 176.410 to 207.774 Ωm cover 14.22 sq km, while those with values between 232.867 and 258.585 Ωm encompass 32.21 sq km, indicating higher groundwater potential. The most promising areas, with GWPI values from 258.586 to 299.987 Ωm, span 27.23 sq km.

Specifically, VES 3 is located within the Oqwashi Asaba Formation, characterized by low aquifer thickness and hydraulic conductivity, yielding the lowest GWPI value. Conversely, VES 10, situated in the Ameki Formation, is known for its low aquifer yield. VES 9, despite being in the Benin Formation, exhibits both the lowest aquifer thickness and coefficient of anisotropy, indicating compacted aquifer materials that significantly limit water yield. This detailed analysis emphasizes the necessity for strategic groundwater management to optimize resource extraction and sustainability

5. Conclusion

This study provides a comprehensive analysis of the geoelectrical characteristics of the aquifer system in Umuahia South and surrounding areas, revealing the presence of four distinct geo-electrical layers with significant variability in resistivity and thickness. The findings demonstrate that the first layer (topsoil) has resistivity values ranging from 2.4 to 191.9 Ωm, with an average of 157.68 Ωm and a mean thickness of 3.72 m. The second layer, composed of clayey sand and sandy clay, shows a resistivity range of 64.4 to 281.4 Ωm and a mean thickness of 6.05 m, while the third layer, primarily consisting of sandstone, exhibits higher resistivity values ranging from 624.3 to 3,209.1 Ωm, with an average of 2,052.01 Ωm. The study highlights that the aquifer system predominantly resides in the third and fourth layers, with resistivity values for the fourth layer between 53.4 and 1,734.3 Ωm.

The results from the VES indicate substantial spatial variability in aquifer properties, with VES points exhibiting the highest and lowest resistivities (VES 6 at 3,209.1 Ωm and VES 9 at 624.3 Ωm, respectively). The investigation also reveals a significant range in aquifer thickness, from 5.2 m to 69.2 m, suggesting a potential for varying groundwater storage capabilities across the region. The analysis of hydraulic conductivity and transmissivity provides further insight into the aquifer's capacity for groundwater movement, with values ranging from 0.207 m/day to 0.954 m/day and transmissivity values from 4.965 m^2/day to 30.441 m^2/day.

This research underscores the importance of understanding the geoelectrical characteristics of aquifers for effective groundwater management and resource planning. The identified areas with favorable conditions for groundwater accumulation and extraction, particularly those exhibiting high hydraulic conductivity and transmissivity, should be prioritized for sustainable water management practices. Conversely, areas with lower resistivity and conductivity may require further investigation to assess their aquifer dynamics and potential for groundwater storage. The findings from this study not only enhance the understanding of the hydrological dynamics in the study area but also provide essential data for future groundwater exploration, conservation efforts, and the sustainable utilization of water resources. Future studies should aim to integrate these geoelectrical findings with hydrological modeling to develop comprehensive groundwater management strategies that account for the region's diverse aquifer characteristics.

Compliance with ethical standards

Disclosure of conflict of interest

No conflict of interest to be disclosed.

References

[1] Abdulrazzaq, Z. T., Agbasi, O. E., Aziz, N. A., & Etuk, S. E. (2020). Identification of potential groundwater locations using geophysical data and fuzzy gamma operator model in Imo, Southeastern Nigeria. Applied Water Science, 10(8). https://doi.org/10.1007/s13201-020-01264-6

[2] Abraham, E., Itumoh, O., Chukwu, C., & Rock, O. (2018). Geothermal Energy Reconnaissance of Southeastern Nigeria from Analysis of Aeromagnetic and Gravity Data. Pure and Applied Geophysics, 176(4), 1615–1638. https://doi.org/10.1007/s00024-018-2028-1

[3] Agbasi, O. E., Aziz, N. A., Abdulrazzaq, Z. T., & Etuk, S. E. (2019). Integrated Geophysical Data and GIS Technique to Forecast the Potential Groundwater Locations in Part of South Eastern Nigeria. Iraqi Journal of Science, 60(5), 1013–1022. https://doi.org/10.24996/ijs.2019.60.5.11

[4] Agharanya, U. P., & Dim, C. I. P. (2018). Water Quality Assessment and Resource Potentials: the Case of Aba–Urban and its Environs, Niger Delta Basin. Water Resources, 45(2), 250–267. https://doi.org/10.1134/s0097807818020161

[5] Akaolisa, C. C., Agbasi, O., Okeke, O. C., & Okechukwu, S. (2022). An assessment of the groundwater potentials of the farm with preliminary geophysical method and grain size analysis prior to the drilling of boreholes. HydroResearch, 5, 85–98. https://doi.org/10.1016/j.hydres.2022.09.001

[6] Akiang, F. B., Amah, E. T., George, A. M., Okoli, E. A., Agbasi, O. E., & Iwuoha, P. O. (2024). Hydrogeological assessment and groundwater potential study in Calabar South Local Government Area: a vertical electrical sounding (VES) approach. International Journal of Energy and Water Resources. https://doi.org/10.1007/s42108-024-00279-y

[7] Akinrinade, O. J., & Adesina, R. B. (2016). Hydrogeophysical investigation of groundwater potential and aquifer vulnerability prediction in basement complex terrain – A case study from Akure, Southwestern Nigeria. Materials and Geoenvironment, 63(1), 55–66. https://doi.org/10.1515/rmzmag-2016-0005

[8] Aleke, C. G., Ibuot, J. C., & Obiora, D. N. (2018). Application of electrical resistivity method in estimating geohydraulic properties of a sandy hydrolithofacies: a case study of Ajali Sandstone in Ninth Mile, Enugu State, Nigeria. Arabian Journal of Geosciences, 11(12). https://doi.org/10.1007/s12517-018-3638-8

[9] Amos-Uhegbu, C. (2014). Geo-electrical Delineation and Geochemical Characteristics of Aquifer Systems in Kwa-Ibo River Watershed, Abia State, Nigeria. Journal of Scientific Research and Reports, 3(6), 818–843. https://doi.org/10.9734/jsrr/2014/6215

[10] Anomohanran, O., Oseme, J. I., Iserhien-Emekeme, R. E., & Ofomola, M. O. (2020). Determination of groundwater potential and aquifer hydraulic characteristics in Agbor, Nigeria using geo-electric, geophysical well logging and pumping test techniques. Modeling Earth Systems and Environment, 7(3), 1639–1649. https://doi.org/10.1007/s40808-020-00888-6

[11] Anosike, S., Ibuot, J. C., Obiora, D. N., & Ugbor, D. O. (2019). Geophysical and physicochemical investigation of groundwater repositories in Njaba LGA of Imo State, eastern Nigeria. International Journal of Environmental Science and Technology, 16(12), 8129–8140. https://doi.org/10.1007/s13762-019-02366-8

[12] Chinye-Ikejiunor, N., Iloegbunam, G. O., Chukwuka, A., & Ogbeide, O. (2021). Groundwater contamination and health risk assessment across an urban gradient: Case study of Onitcha metropolis, south-eastern Nigeria. Groundwater for Sustainable Development, 14, 100642. https://doi.org/10.1016/j.gsd.2021.100642

[13] Ejepu, J. S., Jimoh, M. O., Abdullahi, S., Abdulfatai, I. A., Musa, S. T., & George, N. J. (2024). Geoelectric analysis for groundwater potential assessment and aquifer protection in a part of Shango, North-Central Nigeria. Discover Water, 4(1). https://doi.org/10.1007/s43832-024-00091-z

[14] Emenike, P. C., Nnaji, C. C., & Tenebe, I. T. (2018). Assessment of geospatial and hydrochemical interactions of groundwater quality, southwestern Nigeria. Environmental Monitoring and Assessment, 190(7). https://doi.org/10.1007/s10661-018-6799-8

[15] Eugene-Okorie, J. O., Obiora, D. N., Ibuot, J. C., & Ugbor, D. O. (2020). Geoelectrical investigation of groundwater potential and vulnerability of Oraifite, Anambra State, Nigeria. Applied Water Science, 10(10). https://doi.org/10.1007/s13201-020-01304-1

[16] Fajana, A. O. (2020). Integrated geophysical investigation of aquifer and its groundwater potential in phases 1 and 2, Federal University Oye-Ekiti, south-western basement complex of Nigeria. Modeling Earth Systems and Environment, 6(3), 1707–1725. https://doi.org/10.1007/s40808-020-00785-y

[17] Fatoba, J., Omolayo, S., & Adigun, E. (2014). Using Geoelectric Soundings for Estimation of Hydraulic Characteristics of Aquifers in the Coastal Area of Lagos, Southwestern Nigeria. International Letters of Natural Sciences, 11, 30–39. https://doi.org/10.18052/www.scipress.com/ilns.11.30

[18] George, N. J., Bassey, N. E., Ekanem, A. M., & Thomas, J. E. (2020). Effects of anisotropic changes on the conductivity of sedimentary aquifers, southeastern Niger Delta, Nigeria. Acta Geophysica, 68(6), 1833–1843. https://doi.org/10.1007/s11600-020-00502-4

[19] Ibuot, J. C., Aka, M. U., Inyang, N. J., & Agbasi, O. E. (2022). Georesistivity and physicochemical evaluation of hydrogeologic units in parts of Akwa Ibom State, Nigeria. International Journal of Energy and Water Resources, 8(1), 111–122. https://doi.org/10.1007/s42108-022-00191-3

[20] Ibuot, J. C., George, N. J., Okwesili, A. N., & Obiora, D. N. (2019). Investigation of litho-textural characteristics of aquifer in Nkanu West Local Government Area of Enugu state, southeastern Nigeria. Journal of African Earth Sciences, 153, 197–207. https://doi.org/10.1016/j.jafrearsci.2019.03.004

[21] Ifeanyichukwu, K. A., Okeyeh, E., Agbasi, O. E., Moses, O. I., & Ben-Owope, O. (2021). Using Geo-electric Techniques for Vulnerability and Groundwater Potential Analysis of Aquifers in Nnewi, South Eastern Nigeria. Journal of Geology Geography and Geoecology, 30(1), 43–52. https://doi.org/10.15421/112105

[22] Igwe, O., Ifediegwu, S. I., & Onwuka, O. S. (2020). Determining the occurrence of potential groundwater zones using integrated hydro-geomorphic parameters, GIS and remote sensing in Enugu State, Southeastern, Nigeria. Sustainable Water Resources Management, 6(3). https://doi.org/10.1007/s40899-020-00397-5

[23] Ijioma, U. D. (2021). Delineating the impact of urbanization on the hydrochemistry and quality of groundwater wells in Aba, Nigeria. Journal of Contaminant Hydrology, 240, 103792. https://doi.org/10.1016/j.jconhyd.2021.103792

[24] Joshua, A. K., John, I. A., Ikechukwu, E. D., & Ebuka, A. O. (2023). Scrutinate proclivity of regional aquifer hydraulic parameters: apriorisms for borehole failures within parts of the middle Benue Trough, Nigeria. Water Practice & Technology, 18(12), 3347–3364. https://doi.org/10.2166/wpt.2023.211

[25] Mgbenu, C. N., & Egbueri, J. C. (2019). The hydrogeochemical signatures, quality indices and health risk assessment of water resources in Umunya district, southeast Nigeria. Applied Water Science, 9(1). https://doi.org/10.1007/s13201-019-0900-5

[26] Nwachukwu, S., Bello, R., & Balogun, A. O. (2019). Evaluation of groundwater potentials of Orogun, South–South part of Nigeria using electrical resistivity method. Applied Water Science, 9(8). https://doi.org/10.1007/s13201-019-1072-z

[27] Odochi, U. B., Iheanyichukwu, O. A., Okechukwu, O. S., Chukwuemeka, I. C., Juliana, O. I., Ifeanyi, O. S., Nkiru, N. C., Osita, I. P., & Emmanuel, A. E. (2024). Hydrogeological assessment and contaminant transport modelling of Enyimba landfill site in Aba, Nigeria. Water Practice & Technology, 19(5), 2108–2124. https://doi.org/10.2166/wpt.2024.122

[28] Okoli, E., Akaolisa, C. C. Z., Ubechu, B. O., Agbasi, O. E., & Szafarczyk, A. (2024). Using VES and GIS-Based DRASTIC Analysis to Evaluate Groundwater Aquifer Contamination Vulnerability in Owerri, Southeastern Nigeria. Ecological Questions, 35(3), 1–27. https://doi.org/10.12775/eq.2024.031

[29] Olayinka, A. I., & Oyedele, E. a. A. (2019). On the Application of Coefficient of Anisotropy as an Index of Groundwater Potential in a Typical Basement Complex of Ado Ekiti, Southwest, Nigeria. Physical Science International Journal, 1–10. https://doi.org/10.9734/psij/2019/v22i130119

[30] Oli, I. C., Ahairakwem, C. A., Opara, A. I., Ekwe, A. C., Osi-Okeke, I., Urom, O. O., Udeh, H. M., & Ezennubia, V. C. (2020). Hydrogeophysical assessment and protective capacity of groundwater resources in parts of Ezza and Ikwo areas, southeastern Nigeria. International Journal of Energy and Water Resources, 5(1), 57–72. https://doi.org/10.1007/s42108-020-00084-3

[31] Onwuka, B. M., & Adesemuyi, E. A. (2019). Spatial Distribution of Soil Bulk Density, Organic Carbon and pH under Different Land Use Systems along Umuahia South Local Government Area of Abia State in South Eastern Nigeria. Notulae Scientia Biologicae, 11(2), 298–303. https://doi.org/10.15835/nsb11210466

[32] Opara, A. I., Edward, O. I., Eyankware, M. O., Akakuru, O. C., Oli, I. C., & Udeh, H. M. (2022). Use of geo-electric data in the determination of groundwater potentials and vulnerability mapping in the southern Benue Trough Nigeria. International Journal of Environmental Science and Technology, 20(8), 8975–9000. https://doi.org/10.1007/s13762-022-04485-1

[33] Opara, A. I., Eke, D. R., Onu, N. N., Ekwe, A. C., Akaolisa, C. Z., Okoli, A. E., & Inyang, G. E. (2020). Geo-hydraulic evaluation of aquifers of the Upper Imo River Basin, Southeastern Nigeria using Dar-Zarrouk parameters. International Journal of Energy and Water Resources, 5(3), 259–275. https://doi.org/10.1007/s42108-020-00099-w

[34] Reijers, T. (2011). Stratigraphy and sedimentology of the Niger Delta. Geologos, 17(3). https://doi.org/10.2478/v10118-011-0008-3

[35] Uchendu, U. I., Kanu, C., Kanu, K. C., & Mpamah, C. I. (2019). Spatial pattern of Land Surface Temperature over Umuahia North and Bende LGA, Abia State, Nigeria. Deleted Journal, 3(2), 210–217. https://doi.org/10.36263/nijest.2019.02.0138

[36] Zacchaeus, O. O., Adeyemi, M. B., Adedeji, A. A., Adegoke, K. A., Anumah, A. O., Taiwo, A. M., & Ganiyu, S. A. (2020). Effects of industrialization on groundwater quality in Shagamu and Ota industrial areas of Ogun state, Nigeria. Heliyon, 6(7), e04353. https://doi.org/10.1016/j.heliyon.2020.e04353